

IR/UV double resonant spectroscopy of the methyl radical: Determination of ν_3 in the $3p_z$ Rydberg state

H. B. Fu, Y. J. Hu, and E. R. Bernstein

Citation: *The Journal of Chemical Physics* **123**, 234307 (2005); doi: 10.1063/1.2135772

View online: <http://dx.doi.org/10.1063/1.2135772>

View Table of Contents: <http://aip.scitation.org/toc/jcp/123/23>

Published by the *American Institute of Physics*

COMPLETELY

REDESIGNED!



**PHYSICS
TODAY**

Physics Today Buyer's Guide
Search with a purpose.

IR/UV double resonant spectroscopy of the methyl radical: Determination of ν_3 in the $3p_z$ Rydberg state

H. B. Fu, Y. J. Hu, and E. R. Bernstein^{a)}

Department of Chemistry, Colorado State University, Fort Collins, Colorado 80523

(Received 20 June 2005; accepted 17 October 2005; published online 20 December 2005)

IR+UV double resonant ion-dip and ion-enhancement spectroscopies are employed to study the ν_3 asymmetric CH stretch vibration fundamental of CH₃ in the ground and $3p_z$ Rydberg electronic states. CH₃ radical is synthesized in the supersonic jet expansion by flash pyrolysis of azomethane (CH₃NNCH₃) prior to the expansion. The Q band of the $3^1_1 3p_z \leftarrow \tilde{X}$ transition of CH₃, not detected by conventional UV resonantly enhanced multiphoton ionization (REMPI) spectroscopy, is determined to lie at 59 898 cm⁻¹ using IR+UV REMPI spectroscopy. Energy of the asymmetric CH stretch of CH₃ in the $3p_z$ Rydberg state, $\nu_3(3p_z)$, is 3087 cm⁻¹, redshifted by ~ 74 cm⁻¹ with respect to ground state $\nu_3(\tilde{X})$. © 2005 American Institute of Physics. [DOI: 10.1063/1.2135772]

I. INTRODUCTION

The methyl radical is an important intermediate in many chemical processes of current environmental and industrial interests. These include atmospheric¹ and interstellar² chemistry, hydrocarbon combustion,³ and chemical-vapor deposition of diamond films.⁴ The methyl radical also serves as a prototype species for the entire family of alkyl radicals and, historically, as a benchmark system for open shell molecular-orbital theory. Because of its fundamental and practical importance, CH₃ has been a target for numerous experimental⁵⁻¹⁵ and theoretical¹⁶⁻¹⁹ studies exploring its structural, reaction, and spectroscopic properties. Extensive efforts have been dedicated to establishing sensitive and selective detection methods for CH₃, as a diagnostic and/or concentration titration technique for various chemical reactions and processes.²⁰⁻²⁵ Its ground- and excited-state dynamics have also been investigated. The (2+1) UV resonantly enhanced multiphoton ionization (REMPI) process, employing the $3p_z(^2A_2')$ or $4p_z(^2A_2')$ Rydberg intermediate state, is a viable detection technique for this species and has enjoyed wide applicability for the study of reactions involving the methyl radical.⁶⁻¹⁰ In several state-resolved studies, infrared-absorption spectroscopy has been shown to be an attractive choice for interrogation of the methyl radical.^{26,27}

CH₃ (D_{3h} symmetry) has four vibrational modes: $\nu_1(a_1')$ symmetric stretch, $\nu_2(a_2'')$ out-of-plane bend, $\nu_3(e')$ degenerate asymmetric stretch, and $\nu_4(e')$ degenerate in-plane bend. Their energies in the ground electronic state $\tilde{X}(^2A_2')$ have been carefully examined by various techniques. The first few ν_2 umbrella mode vibrational bands of both CH₃ (Ref. 15) and CD₃ (Ref. 28) have been recorded and analyzed by diode laser spectroscopy. The higher-energy ν_3 fundamental band has been investigated employing a difference frequency laser.¹⁴ The infrared inactive ν_1 symmetric stretch has been examined employing the coherent anti-Stokes Raman spectroscopy (CARS) technique.²⁹ All two-photon spectra of the

$3p_z \leftarrow \tilde{X}$ transition seem to be dominated by the 0_0^0 , 2_1^1 , and 2_0^2 features and previous spectra of the $3p_z$ or $4p_z$ Rydberg states do not evidence any vibrations of e' symmetry (ν_3, ν_4).⁶⁻¹⁰ Selection rules for multiphoton spectroscopy do not forbid any of the four fundamental vibrations from being detected,^{6,30} but the ν_2 mode must be obtained as a hot transition or an overtone. Most recently, Liu and co-workers reported detection of the 1_1^1 , 3_1^1 , and $4_1^1 3p_z \leftarrow \tilde{X}$ transitions of CD₃ produced from a F+CHD₃ crossed-beam reaction using REMPI spectroscopy.^{24,25} These authors deduced the $\nu_3(3p_z)$ of CH₃=3114 cm⁻¹ based on the isotope shift of the ground state,²⁵ about 100 cm⁻¹ smaller than the calculated value of $\nu_3(3p_z)=3210$ cm⁻¹ for CH₃ reported by Mebel and Lin.¹⁸

In order to understand the energy levels and dynamics for the methyl radical, the energies of the vibrational modes in the $3p_z$ and $4p_z$ Rydberg states are needed. In this report, three separate experiments are designed to observe and assign the $3^1_1 3p_z \leftarrow \tilde{X}$ transition of CH₃ and thereby to determine a value for the $\nu_3(3p_z)$ vibrational mode. First, employing the IR+UV double resonant ion-dip (DRID-IR) technique, $\nu_3(\tilde{X})$ is recorded by the depletion of CH₃⁺ ion signal obtained from (2+1) REMPI spectroscopy via the $4p_z$ electronic state whenever IR absorption to $\nu_3(\tilde{X})$ occurs. Second, IR+UV REMPI spectroscopy is utilized to identify the $3^1_1 3p_z \leftarrow \tilde{X}$ transition by scanning the UV laser energy with the IR laser wavelength fixed at the maximum absorption found by DRID-IR. Third, IR+UV double resonant ion-enhancement (DRIE-IR) spectroscopy is developed based on the optical selection rules of CH₃ in D_{3h} symmetry, and achieved by scanning the IR laser frequency with the UV laser frequency fixed at the Q band of the $3^1_1 3p_z \leftarrow \tilde{X}$ transition. DRIE-IR spectra are detected by the increase of CH₃⁺ intensity because the $\nu_3(\tilde{X})$ vibrationally excited CH₃ radicals can be selectively ionized by the UV radiation via the $\nu_3(3p_z)$ state. The success of DRIE-IR spectroscopy confirms the assignment of the $3^1_1 3p_z \leftarrow \tilde{X}$ transition located by the IR+UV REMPI spectroscopy. The Q band of the

^{a)}Electronic mail: erb@lamar.colostate.edu

$3_1^1 3p_z \leftarrow \tilde{X}$ transition of CH_3 is redshifted from the Q band of the $0_0^0 3p_z \leftarrow \tilde{X}$ transition by $\sim 74 \text{ cm}^{-1}$. The $\nu_3(3p_z)$ is calculated to be $\sim 3087 \text{ cm}^{-1}$.

II. EXPERIMENTAL PROCEDURES

Methyl radicals are produced by pyrolysis of azomethane (CH_3NNCH_3) prior to supersonic expansion. Azomethane is synthesized according to published procedures^{31,32} and stored in a stainless-steel cylinder at room temperature. A hyperthermal pulsed nozzle source, modeled after the design by Chen *et al.* with some modifications, is employed for the expansion.^{10,33} The optimized pyrolysis temperature for azomethane is 1100 K.

A gas mixture of $\sim 0.5\%$ azomethane and $\sim 99.5\%$ argon at a backing pressure of ~ 50 psi is expanded through the orifice of the pulsed valve into the SiC tube. The temperature in the heating zone is high enough so that nearly all the azomethane is decomposed to CH_3 and N_2 . The sample contact time in the heating zone is estimated to be $\sim 30 \mu\text{s}$, short enough to suppress radical-radical reactions.³³ Subsequent supersonic expansion into vacuum chamber cools CH_3 to ~ 50 K rotational temperature by collision with inert carrier gas. Since only molecular nitrogen is produced as a by-product of this decomposition reaction, flash pyrolysis of azomethane with subsequent supersonic cooling provides a clean source of methyl radicals.

Tunable IR radiation from 3000 to 3450 cm^{-1} , produced in an optical parametric oscillator (OPO, Laser Vision) pumped by a 10 Hz Nd/YAG (yttrium aluminum garnet) laser (532 nm), is used to excite the radical to a selected vibrational level in the ground electronic state. The IR radiation has a pulse energy of 15 mJ with a full width at half maximum (FWHM) pulse length of ~ 10 ns and a bandwidth of $\sim 3 \text{ cm}^{-1}$. The IR radiation is focused into the core of the skimmed supersonic beam using a 40 cm focal length lens. The output of a frequency-doubled dye laser (Spectra Physics) pumped by a frequency-doubled Nd/YAG laser (Spectra Physics) is focused coaxially to the same jet region by a 50 cm focal length lens from the opposite direction. (2+1) REMPI transitions for $3p_z$ and $4p_z$ intermediate states are generated by a tunable dye laser employing a mixture of DCM and LDS 698 ($3p_z$) and Rhodamine 590 ($4p_z$) as the active medium. The relative time between IR and UV laser pulses is controlled by a digital delay generator (SRS, DG535). Optimum signal is obtained for zero time delay between the two laser pulses. Laser wavelengths (vacuum) are calibrated as known IR and UV molecular transitions in appropriate spectral regions.

Ions created by the ionization (dye) laser are extracted from the ionization region of the time-of-flight mass spectrometer (TOFMS) at 4 keV total energy. Mass-resolved detection is achieved by using a Galileo Electro-Optics microchannel plate (MCP) at the end of a 1.5 m flight tube. The data-acquisition scheme for the infrared spectroscopy is similar to that we used to record REMPI spectroscopy described in details from this laboratory.^{34,35} IR+UV double resonant ionization spectroscopy has been exploited widely in studying IR absorption of molecules^{36,37} and radicals.³⁸

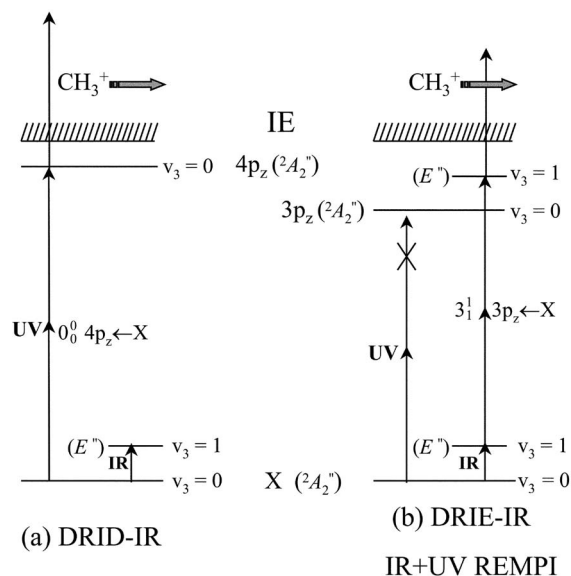


FIG. 1. Energetic diagrams of (a) DRID-IR and (b) DRIE-IR and IR+UV REMPI spectroscopies. The symbols in the parentheses indicate the overall vibronic symmetry of corresponding state. See text for the assignment of the $3_1^1 3p_z \leftarrow \tilde{X}$ transition.

Figure 1 illustrates the energetic diagrams of (a) DRID-IR and (b) DRIE-IR and IR+UV REMPI spectroscopies for CH_3 radicals.

III. RESULTS

The initially resolved gas-phase IR single-photon $\nu_3(\tilde{X})$ spectrum of CH_3 was first recorded and analyzed by Amano *et al.* using a difference frequency laser and Zeeman modulation absorption spectroscopy.¹⁴ The ν_3 vibrational mode of CH_3 is doubly degenerate and has vibrational angular momentum $l=1$ with overall vibronic symmetry $\Psi_e\Psi_v=E''$ in the electronic ground state $\tilde{X}(^2A_2'')$. Figure 2(a) displays the

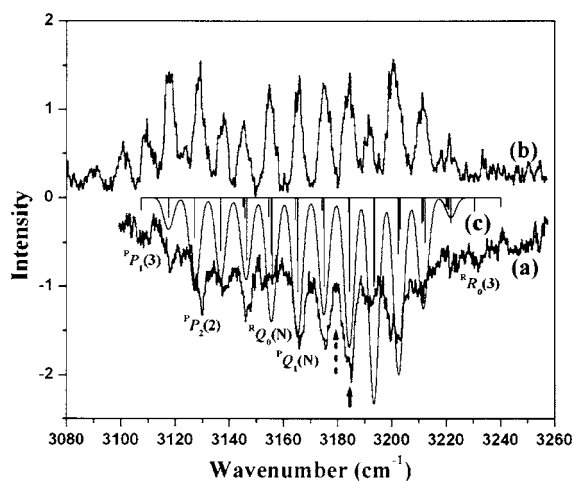


FIG. 2. The $\nu_3(\tilde{X})$ asymmetric CH stretch spectra of CH_3 in the fundamental region recorded by (a) DRID-IR and (b) DRIE-IR spectroscopies with the UV laser fixed at 34927 and 29949 cm^{-1} to reach the $0_0^0 4p_z \leftarrow \tilde{X}$ and the $3_1^1 3p_z \leftarrow \tilde{X}$ transitions, respectively. Curve (c) shows the theoretically calculated spectrum with $T_{\text{rot}} \sim 50$ K. Stick plot represents the calculated bands with relative intensities. The solid and dashed arrows indicate the IR laser frequencies used in the IR+UV REMPI experiment (see text for details).

TABLE I. Optical selection rules for CH₃ transitions with different initial and final state vibronic symmetries.

Vibronic state symmetry ($\Psi_e \Psi_v$)		Numbers of absorbed identical photons		
Initial	Final	One photon	Two photon	
A_2''	A_2''	Forbidden	$\Delta K=0$ For $K=0$, $\Delta N=0, \pm 2$ For $K \neq 0$, $\Delta N=0, \pm 1, \pm 2$	
A_2''	E''	$\Delta K=\Delta l=\pm 1$ $\Delta N=0, \pm 1$	or $\Delta G=0^a$	$\Delta K=2(-\Delta l)=\pm 2$ $\Delta N=0, \pm 1, \pm 2$
E''	E''	Forbidden	$\Delta K=0$ For $K=0$, $\Delta N=0, \pm 2$ For $K \neq 0$, $\Delta N=0, \pm 1, \pm 2$	
E''	A_2''	$\Delta K=\Delta l=\pm 1$ $\Delta N=0, \pm 1$	or $\Delta G=0^a$	$\Delta K=2(-\Delta l)=\pm 2$ $\Delta N=0, \pm 1, \pm 2$

^a G has been defined as $G=l-k$, with $K=|k|$. k is the projection of the total angular momentum along the molecule-fixed z axis (top axis).

$\nu_3(\tilde{X})$ spectrum of CH₃ recorded by the DRID-IR spectroscopy. Although the high level of background CH₃⁺ signal produced by the UV laser decreases the S/N ratio, DRID-IR spectrum (using the $0_0^0 4p_z \leftarrow \tilde{X}$ transition as part of the detection chain) still exhibits well-resolved rotational structure. Employing the rotational constants determined by Amano *et al.*,¹⁴ the $\nu_3(\tilde{X})$ fundamental of CH₃ is simulated as displayed in Fig. 2(c); in the modeling, higher-order parameters of the rotational Hamiltonian (e.g., centrifugal distortion, spin-rotation interaction, etc.) are set to zero, and rotational lines are convolved with a Gaussian width of 3 cm⁻¹ (the IR laser bandwidth). Trace (c) is in good agreement with the DRID-IR spectrum [trace (a)]. The band origin of $\nu_3(\tilde{X})$ at ~ 3161 cm⁻¹ is consistent with the published value of $\nu_3(\tilde{X})=3160.821$ cm⁻¹.¹⁴ An acceptable fit within our S/N ratio is obtained using $T_{\text{rot}} \sim 50$ K, similar to the value estimated from (2+1) REMPI spectrum via the $3p_z$ state.¹⁰ The simulation results are also given as a stick plot in Fig. 2(c). Clearly, each single peak in the DRID-IR spectrum (at current resolution) contains many rotation transitions. As shown in Table I, selection rules for the $\nu_3(\tilde{X}) \leftarrow 0(\tilde{X}) [E'' \leftarrow A_2'']$ single-photon transition are $\Delta N=0, \pm 1$, $\Delta K=\pm 1$, and $\Delta l = \pm 1$, or $\Delta G=0$.^{39,40} Examples of assignments are labeled in the traditional $^{\Delta K} \Delta N_K(N)$ manner in Fig. 2. The absence of $^Q Q_K(N)$ transitions results from the planar geometry of CH₃ in D_{3h} point group. Since the $\nu_3(\tilde{X}) \leftarrow 0(\tilde{X}) [E'' \leftarrow A_2'']$ band is perpendicular (a pure b -type band), the subband origins depend strongly on K . For example, peak positions of $^R Q_0(N)$ and $^P Q_1(N)$ in Fig. 2 depend on K value and vary little with N value.

The dashed line in Fig. 3 depicts the conventional (2+1) REMPI spectrum of CH₃ in the vicinity of the $0_0^0 3p_z \leftarrow \tilde{X}$ transition. The general appearance of this spectrum is consistent with that reported previously^{9,10,24,25}—a dominant Q branch with rotational-resolved P , Q , R , and S (not shown in Fig. 3) branches on either side. The value of the wave number in Fig. 3 is in vacuum, and the Q band of the $0_0^0 3p_z \leftarrow \tilde{X}$ transition is 59 972 cm⁻¹ according to Refs. 6, 41, and 42. The solid line spectrum in Fig. 3 is the IR+UV

REMPI spectrum recorded by scanning the UV laser energy with the IR laser energy fixed at 3184 cm⁻¹ as indicated in Fig. 2 by the solid arrow. As compared with the conventional UV REMPI spectrum, a new feature, centered at 59 898 cm⁻¹, is observed to overlap the $P(4)$ band of the $0_0^0 3p_z \leftarrow \tilde{X}$ transition and redshift from the Q band of the $0_0^0 3p_z \leftarrow \tilde{X}$ transition by ~ 74 cm⁻¹ using the IR+UV REMPI spectroscopy. Meanwhile, other rotational structures belonging to the $0_0^0 3p_z \leftarrow \tilde{X}$ transition (UV REMPI) remain the same. This new IR+UV REMPI feature has a FWHM of ~ 9 cm⁻¹, similar to the Q band of the $0_0^0 3p_z \leftarrow \tilde{X}$ transition, but broader than other rotational features of the $0_0^0 3p_z \leftarrow \tilde{X}$ transition (typical FWHM ~ 5 cm⁻¹). The IR+UV REMPI feature at 59 898 cm⁻¹ is not observed if the IR laser radiation is absent or if the IR frequency is changed from 3184 to 3179 cm⁻¹, i.e., from a peak position to an off-peak position as indicated in Fig. 2 by the solid (on) and dashed

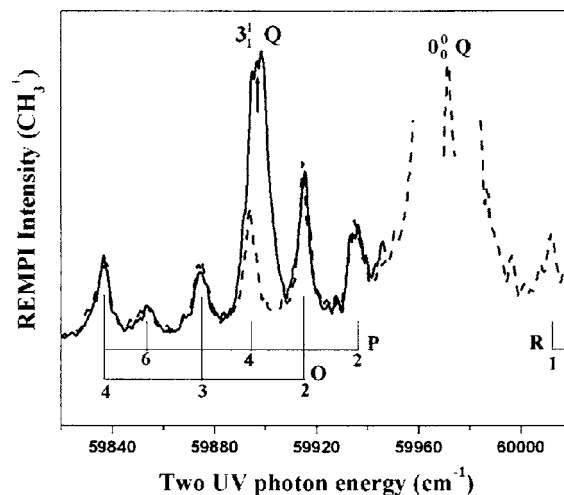


FIG. 3. The conventional UV REMPI (dashed line) and IR+UV REMPI (solid line) spectra of CH₃ in the vicinity of the $0_0^0 3p_z \leftarrow \tilde{X}$ transition. The intense Q band of the $0_0^0 3p_z \leftarrow \tilde{X}$ transition is broken off in order to display the weaker P , R , and O branches. The arrow points to the Q band of the $3_1^1 3p_z \leftarrow \tilde{X}$ transition.

(off) arrows. This clarifies that the IR+UV REMPI detected transition arises from $\nu_3(\tilde{X})$ vibrationally excited CH_3 induced by IR excitation.

The initial state for this IR+UV REMPI process is $\nu_3(\tilde{X})$, which has $A_2'' \times e' = E''$ vibronic symmetry. For an allowed two-photon (from the same laser) transition, both A_2'' and E'' final vibronic states are accessible for the methyl radical. In this regard, $\nu_1(3p_z)$, $\nu_3(3p_z)$, and $\nu_4(3p_z)$ can be candidates for the final state with vibronic symmetries of A_2'' , E'' , and E'' , respectively. Two-photon selection rules (see Table I) for perpendicular bands, such as the $\nu_1(3p_z) \leftarrow \nu_3(\tilde{X}) [A_2'' \leftarrow E'']$ transition, generally produce a congested spectrum; in particular, the very strong Q branch observed for parallel bands is not expected. All of CH_3 previous spectroscopy studies do not observe the $\nu_3(3p_z) \leftarrow 0(\tilde{X}) [E'' \leftarrow A_2'']$ transition, which is a cold band and shares the same selection rules as the $\nu_1(3p_z) \leftarrow \nu_3(\tilde{X}) [A_2'' \leftarrow E'']$ transition. Moreover, the energy difference between $\nu_3(\tilde{X})$ and $\nu_1(3p_z)$ is $59\,725\text{ cm}^{-1}$, according to $1_0^1 - \nu_3(\tilde{X})$ with $1_0^1(3p_z \leftarrow \tilde{X}) = 62\,886\text{ cm}^{-1}$ reported by Hudgens *et al.*⁶ and $\nu_3(\tilde{X}) = 3161\text{ cm}^{-1}$, far away from the IR+UV REMPI detected band at $59\,898\text{ cm}^{-1}$. Thus the $\nu_1(3p_z)$ is excluded as a possible final state for the $3p_z \leftarrow \tilde{X}$ IR+UV transition. On the other hand, a transition from $\nu_3(\tilde{X})$ (asymmetric stretch) to $\nu_4(3p_z)$ (degenerate in-plane bend) is not expected, on theoretical grounds,¹⁸ to have a large Franck-Condon factor. Based on the harmonic approximation, a recent *ab initio* calculation indicates that the diagonal transitions x_1^1 of all four CH_3 vibrational modes ($\nu_x, x=1, \dots, 4$) for the $3p_z \leftarrow \tilde{X}$ transition should exhibit large Franck-Condon factors in the (2+1) REMPI scheme.²⁵ Most recently, Liu and co-workers reported detection of the 1_1^1 , 3_1^1 , and $4_1^1 3p_z \leftarrow \tilde{X}$ transitions of CD_3 .^{24,25} Therefore, the IR+UV REMPI detected transition at $59\,898\text{ cm}^{-1}$ is assigned to the Q band of the $3_1^1 3p_z \leftarrow \tilde{X}$ transition of CH_3 .

The IR energy can be fixed at any peak position displayed in the DRID-IR spectrum in Fig. 2(a), and the Q band of the $3_1^1 3p_z \leftarrow \tilde{X}$ transition observed in IR+UV experiments remains within the range of $59\,898 \pm 1\text{ cm}^{-1}$. This circumstance arises because of the selection rules presented in Table I for the $\nu_3(\tilde{X}) \leftarrow 0(\tilde{X}) [E'' \leftarrow A_2'']$ IR single-photon transition and for the $\nu_3(3p_z) \leftarrow \nu_3(\tilde{X}) [E'' \leftarrow E'']$ UV two-photon transition. The $\Delta K=0$ selection rule for the $3_1^1 3p_z \leftarrow \tilde{X}$ transition generates a very strong Q branch if the rotational constants of CH_3 in the lower \tilde{X} and upper $3p_z$ states do not differ significantly [$\Delta B(\text{CD}_3) = 4.76(3p_z) - 4.80(\tilde{X}) = 0.04\text{ cm}^{-1}$].⁴³ Contributions from each K component fall at nearly the same energy for each particular transition ($\Delta N=0, \pm 1, \pm 2$). Only the intense Q band of the $3_1^1 3p_z \leftarrow \tilde{X}$ transition can be detected in the IR+UV REMPI experiment. Since the energy of this transition is determined by the difference between $\nu_3(\tilde{X})(K, N)$ and $\nu_3(3p_z)(K, N)$ levels, the $\Delta K=0=\Delta N$ selection rule makes this energy ($59\,898\text{ cm}^{-1}$) insensitive to K or N values. Therefore, the Q band of the $3_1^1 3p_z \leftarrow \tilde{X}$ transition always appears at $59\,898\text{ cm}^{-1}$ in IR+UV REMPI experi-

ment, redshifted from the Q band of the $0_0^0 3p_z \leftarrow \tilde{X}$ transition by $\sim 74\text{ cm}^{-1}$, no matter which (K, N) levels of $\nu_3(\tilde{X})$ are populated by IR excitation. This leads to the development of DRIE-IR spectroscopy for CH_3 . Figure 2(b) is the $\nu_3(\tilde{X})$ spectrum of CH_3 recorded by DRIE-IR spectroscopy. Features shown in DRIE-IR spectrum correspond well to those identified in the depletion spectrum [Fig. 3(a)]. UV radiation at $29\,949\text{ cm}^{-1}$ is not resonant for $0(\tilde{X}) \text{CH}_3$ radicals, thus DRIE-IR spectrum has nearly a zero background. The success of DRIE-IR experiment further confirms the assignment of the new band at $59\,898\text{ cm}^{-1}$ in IR+UV REMPI spectrum to the Q band of the $3_1^1 3p_z \leftarrow \tilde{X}$ transition of CH_3 .

IV. DISCUSSION

The Q band of the $3_1^1 3p_z \leftarrow \tilde{X}$ transition of CH_3 identified by the IR+UV REMPI spectroscopy is redshifted from the Q band of the $0_0^0 3p_z \leftarrow \tilde{X}$ transition by $\sim 74\text{ cm}$, overlapping the $P(4)$ band of the $0_0^0 3p_z \leftarrow \tilde{X}$ transition. Note that the Q band of the $1_1^1 3p_z \leftarrow \tilde{X}$ transition of CH_3 reported by Epstein and Parker²³ and Liu and co-workers^{24,25} also overlaps the $P(4)$ band of the $0_0^0 3p_z \leftarrow \tilde{X}$ transition. Because of the spectral broadening as a result of the predissociative nature of the $3p_z$ state, the Q bands of the 3_1^1 and $1_1^1 3p_z \leftarrow \tilde{X}$ transitions of CH_3 may both overlap the $P(4)$ band of the $0_0^0 3p_z \leftarrow \tilde{X}$ transition. In our DRIE-IR experiment, $0(\tilde{X}) \text{CH}_3$ radicals are excited to the $\nu_3(\tilde{X})$ state by the IR laser, but $0(\tilde{X}) \text{CH}_3$ cannot be populated to the $\nu_1(\tilde{X})$ state because $\nu_1(\tilde{X})$ is IR inactive.²⁹ The IR+UV REMPI detected feature at $59\,898\text{ cm}^{-1}$ belongs to the Q band of the $3_1^1 3p_z \leftarrow \tilde{X}$ transition of CH_3 , redshifted by $\sim 74\text{ cm}^{-1}$ with respect to the Q band of the $0_0^0 3p_z \leftarrow \tilde{X}$ transition at $59\,972\text{ cm}^{-1}$.

$\nu_3(3p_z)$ of CH_3 is calculated at 3087 cm^{-1} according to $\nu_3(3p_z) = \nu_3(\tilde{X}) + (3_1^1 - 0_0^0)$, with $\nu_3(\tilde{X}) = 3161\text{ cm}^{-1}$ and $(3_1^1 - 0_0^0) = -74\text{ cm}^{-1}$. One would initially think that all these experiments, DRID-IR, DRIE-IR, and IR+UV REMPI, could have been carried out for the $3p_z \leftarrow \tilde{X}$ transition to obtain the $\nu_3(3p_z)$ more directly. Nonetheless, the DRID-IR technique only works for the $0_0^0 4p_z \leftarrow \tilde{X}$ transition and the DRIE-IR only works for the $3_1^1 3p_z \leftarrow \tilde{X}$ transition. The transitions that remain undetected (for a $S/N > 1$) are the $3_1^1 4p_z \leftarrow \tilde{X}$ DRIE-IR transition and the $0_0^0 3p_z \leftarrow \tilde{X}$ DRID-IR transition. Problems dealing with dynamics ($4p_z$), cross sections, and background ($3p_z$) may be the cause of these missing processes.

A final point concerns the techniques used in the present study of CH_3 . The IR+UV DRID-IR depletion scheme exploits the known Franck-Condon factor for the UV transition and functions as a standard procedure that can be applied for different targets. In IR+UV DRIE-IR, as the IR-excited rovibronic state changes, UV excitation of the IR-populated rovibronic state to Frank-Condon favored levels in the upper electronic state also changes. One would initially think that IR and UV laser frequencies have to be tuned simultaneously to acquire the IR+UV DRIE-IR spectrum, as was reported

for the study of hydroxymethyl radical.³⁸ Limited by the symmetry of CH₂OH, the energy of the UV transition for DRIE-IR is different if different rovibronic levels in the ground electronic state are prepared by IR radiation.³⁸ CH₃ has a planar geometry with D_{3h} symmetry, however, no matter which K or N levels in $\nu_3(\tilde{X})$ are populated by IR radiation; the UV transition used in DRIE-IR, i.e., the Q band of the $3_1^1 3p_z \leftarrow \tilde{X}$ transition, does not change position. Our results demonstrate that IR+UV REMPI combined with DRIE-IR spectroscopy provides an important mechanism for observing and assigning new vibronic transitions that are inaccessible by conventional REMPI from the $0(\tilde{X})$ state.

ACKNOWLEDGMENTS

This work was supported by grants from U.S. NSF and in part by Philip Morris USA Inc. and Philip Morris International through the Research Management Group.

- ¹R. P. Wayne, *Chemistry of Atmospheres* (Oxford University Press, Oxford, 2000).
- ²H. Suzuki, *Prog. Theor. Phys.* **62**, 936 (1979).
- ³J. A. Miller, R. J. Kee, and C. K. Westbrook, *Annu. Rev. Phys. Chem.* **41**, 345 (1990).
- ⁴F. G. Celii and J. E. Butler, *Annu. Rev. Phys. Chem.* **42**, 643 (1991).
- ⁵G. Herzberg, *Proc. R. Soc. London, Ser. A* **262**, 291 (1961).
- ⁶J. W. Hudgens, T. G. DiGiuseppe, and M. C. Lin, *J. Chem. Phys.* **79**, 571 (1983).
- ⁷T. G. DiGiuseppe, J. W. Hudgens, and M. C. Lin, *J. Chem. Phys.* **86**, 36 (1982).
- ⁸J. L. Brum, R. D. Johnson III, and J. W. Hudgens, *J. Chem. Phys.* **98**, 3732 (1993).
- ⁹J. F. Black and I. Powis, *J. Chem. Phys.* **89**, 3986 (1988).
- ¹⁰P. Chen, S. D. Colson, W. A. Chupka, and J. A. Berson, *J. Phys. Chem.* **90**, 2319 (1986).
- ¹¹J. A. Blush, P. Chen, R. T. Wiedmann, and M. G. White, *J. Chem. Phys.* **98**, 3557 (1993).
- ¹²M. N. R. Ashfold, S. G. Clement, J. D. Howe, and C. M. Western, *J. Chem. Soc., Faraday Trans.* **89**, 1153 (1993).
- ¹³S. G. Westre, P. B. Kelly, Y. P. Zhang, and L. D. Ziegler, *J. Chem. Phys.*

- 94**, 270 (1991).
- ¹⁴T. Amano, P. F. Bernath, C. Yamada, Y. Endo, and E. Hirota, *J. Chem. Phys.* **77**, 5284 (1982).
- ¹⁵C. Yamada, E. Hirota, and K. Kawaguchi, *J. Chem. Phys.* **75**, 5256 (1981).
- ¹⁶P. Botschwina, J. Flesch, and W. Meyer, *Chem. Phys.* **74**, 321 (1983).
- ¹⁷A. M. Velasco, I. Martin, and C. Lavin, *Chem. Phys. Lett.* **264**, 579 (1997).
- ¹⁸A. M. Mebel and S. H. Lin, *Chem. Phys.* **215**, 329 (1997).
- ¹⁹K. M. Chen, *J. Chem. Phys.* **119**, 7163 (2003).
- ²⁰J. J. Scherer, K. W. Aniolek, N. P. Cernansky, and D. J. Rakestraw, *J. Chem. Phys.* **107**, 6196 (1997).
- ²¹H. Kojima, H. Toyoda, and H. Sugai, *Appl. Phys. Lett.* **55**, 1292 (1989).
- ²²Z. H. Kim, H. A. Bechtel, J. P. Camden, and R. N. Zare, *J. Chem. Phys.* **122**, 084303 (2005).
- ²³A. T. J. B. Eppink and D. H. Parker, *J. Chem. Phys.* **110**, 832 (1999).
- ²⁴W. Shiu, J. J. Lin, and K. Liu, *Phys. Rev. Lett.* **92**, 103201 (2004).
- ²⁵B. Zhang, J. Zhang, and K. Liu, *J. Chem. Phys.* **122**, 104310 (2005).
- ²⁶K. Sugawara, F. Ito, T. Nakanaga, H. Takeo, and C. Masumura, *J. Chem. Phys.* **92**, 5328 (1990).
- ²⁷T. Suzuki and E. Hirota, *J. Chem. Phys.* **98**, 2387 (1993).
- ²⁸J. M. Frye, T. J. Sears, and D. Leitner, *J. Chem. Phys.* **88**, 5300 (1988).
- ²⁹P. L. Holt, K. E. McCurdy, R. B. Weisman, J. S. Adams, and P. S. Engel, *J. Chem. Phys.* **81**, 3349 (1984).
- ³⁰K. Chen and E. S. Yeung, *J. Chem. Phys.* **69**, 43 (1978).
- ³¹R. Renaud and L. C. Leitch, *Can. J. Phys.* **32**, 545 (1954).
- ³²S. Nandi, S. J. Blanksby, X. Zhang, M. R. Nimlos, D. C. Dayton, and G. B. Ellison, *J. Phys. Chem. A* **106**, 7547 (2002).
- ³³X. Zhang, A. V. Friderichsen, S. Nandi, G. B. Ellison, D. E. David, J. T. McKinnon, T. G. Lindeman, D. C. Dayton, and M. R. Nimlos, *Rev. Sci. Instrum.* **74**, 3077 (2003).
- ³⁴R. Disselkamp and E. R. Bernstein, *J. Chem. Phys.* **98**, 4339 (1993).
- ³⁵E. R. Bernstein, K. Law, and M. Schauer, *J. Chem. Phys.* **80**, 207 (1984).
- ³⁶R. H. Page, Y. R. Shen, and Y. T. Lee, *J. Chem. Phys.* **88**, 5362 (1988).
- ³⁷M. Hippler, R. Pfab, and M. Quack, *J. Phys. Chem. A* **107**, 10743 (2003).
- ³⁸L. Feng, J. Wei, and H. Reisler, *J. Phys. Chem. A* **108**, 7903 (2004).
- ³⁹G. Herzberg, *Molecular Spectra and Molecular Structure* (Van Nostrand Reinhold, New York, 1966), Vol. III.
- ⁴⁰J. T. Hougen, *J. Chem. Phys.* **37**, 1433 (1962).
- ⁴¹M. E. Jacox, *J. Phys. Chem. Ref. Data* **32**, 1 (2003).
- ⁴²The NIST Chemistry Webbook, <http://webbook.nist.gov/chemistry>
- ⁴³D. H. Parker, Z. W. Wang, M. H. M. Janssen, and D. M. Chandler, *J. Chem. Phys.* **90**, 60 (1989).